Biocatalysis and Agricultural Biotechnology 18 (2019) 101036

Contents lists available at ScienceDirect

Biocatalysis and Agricultural Biotechnology

journal homepage: www.elsevier.com/locate/bab

Growth, morphology and bioactive phenolic compounds production in *Pyrostegia venusta* calli

Mairon César Coimbra, Rafael César Russo Chagas, Marlúcia Souza Pádua Vilela, Ana Hortência Fonsêca Castro*

Laboratório de Farmacobotânica e Plantas Medicinais, Universidade Federal de São João del-Rei (UFSJ), Campus Centro-Oeste, Rua Sebastião Gonçalves Coelho, 400, Chanadour, 35501-296, Divinópolis, MG, Brazil

ARTICLE INFO

Keywords:
Phenolics
Flavonoids
In vitro cultures
Medicinal plant
Brazilian Cerrado

ABSTRACT

Pyrostegia venusta is a medicinal climbing plant commonly used in traditional Brazilian medicine to treat diarrhea, vitiligo, cough and common infections. In order to evaluate the growth, morphology and bioactive phenolic compounds production in *P. venusta* calli, cultures were established on MS medium supplemented with 4.52 µM of 2,4-dichlorophenoxyacetic acid and 8.88 µM 6-benzylaminopurine in the absence of light. Morphological analyses were performed with scanning and transmission electron microscopy. Total proteins, amino acids, soluble and reducing sugars, phenols, and flavonoids contents were quantified by spectrophotometric assays, and the phenolic compounds profile was evaluated by high-performance liquid chromatography. The calli growth showed a sigmoidal pattern, with four distinct phases: *lag*, exponential, linear and decline phases. Ultrastructural analysis showed cells with meristematic characteristics at the start of the culture (*lag* and exponential phases), cellular organizations in clusters in the linear phase and ruptured cells without visible organelles in the decline phase. The highest levels of primary metabolites (proteins, amino acids, soluble and reducing sugars) and secondary metabolites (phenols and flavonoids) were observed at 10 days of culture (*lag* phase) and in general decreased with callus growth. Benzoic and *p*-coumaric acid derivatives and rutin were observed in the initial explant, and caffeic acid derivatives were detected in the callus culture at 60 and 120 days.

1. Introduction

Pyrostegia venusta (Ker Gawl.) Miers, also known as "orange trumpet" or "cipó-de-são-joão" is a liana creeper (Fig. 1A–B) found in south and southeast Brazil (Duarte and Jurgensen, 2007). In folk medicine, leaves and flowers are used to treat diarrhea, vitiligo, cough and common infections of the respiratory system such as bronchitis, flu and cold (Ferreira et al., 2000; Scalon et al., 2008; Cardozo et al., 2009). Its use in folk medicine has been confirmed by several studies that confirm the antioxidant, antimicrobial and wound healing activities (Roy et al., 2011, 2012; Silva et al., 2011). Other biological activities such as improvement of symptoms of flu and cold, anti-inflammatory and antinociceptive effects are also observed by Veloso et al. (2010, 2012, 2014). Moreira et al. (2012, 2105) reported the use of *P. venusta* flowers to treat vitiligo by the stimulation of melanogenesis. These biological activities are related to phenolic compounds, mainly flavonoids.

In vitro cell culture of *P. venusta* is an important source for production of bioactive compounds (Loredo-Carrillo et al., 2012; Braga et al., 2015; Coimbra et al., 2017), since the main problems for the species propagation are the seasonal production of seeds and the low percentage of germination (Rossatto and Kolb, 2010; Braga et al., 2015). *In vitro* plant cell culture, especially callus culture, allows continuous production of bioactive compounds in a short time and more flexible culture cycles; in addition, cells are free of diseases and are not exposed to seasonal variations, and it is possible to discover products not yet found in nature (Murthy et al., 2014; Isah et al., 2018).

Studies about callus growth and morphology are important to identify the stages where the fundamental processes related to the growth and development of cultures occur. From this point, we can optimize the conditions for *in vitro* culture, define the exact time of subculture of calli to a new medium or use it to produce bioactive compounds in medicinal species (Smith, 2013). Furthermore, to know the biochemical profile of the cultures, such as protein, amino acids and sugars contents can aid in the early identification of morphogenic processes that occur during cellular differentiation, growth, and

* Corresponding author.
E-mail address: acastro@ufsj.edu.br (A.H.F. Castro).

https://doi.org/10.1016/j.bcab.2019.101036
Received 14 December 2018; Received in revised form 4 February 2019; Accepted 7 February 2019
Available online 08 February 2019
1878-8181/

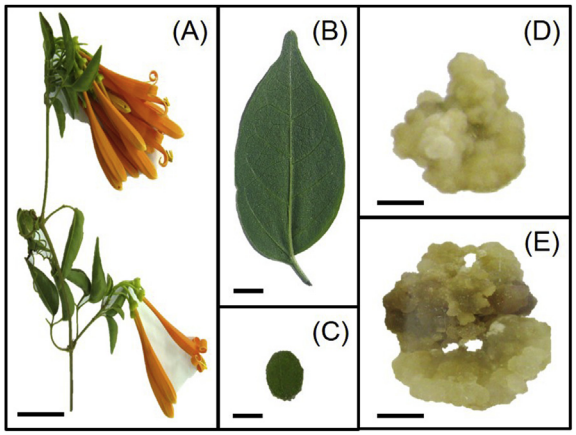

Fig. 1. *Pyrostegia venusta*: (**A**) fertile branches; (**B**) leaf - source of explants for *in vitro* culture; (**C**) initial explant - fragment of the source leaf of explants; (**D**) callus with 30 days of culture; (**E**) callus with 90 days of culture. *Scale bars*: 3 cm (**A**); 0.5 cm (**B,C,D,E**).

propagation in plants (Piza et al., 2003; Santos et al., 2011). Also, ultrastructural analysis allows the verification of morphological aspects related with embryogenic characteristics, enabling the early selection of embryogenic cells while reducing cost, time and labor (Ribeiro et al., 2012; Pádua et al., 2013).

Auxins and cytokinins are usually employed in callus induction (Coenen and Lomax, 1997), and high auxin concentrations or a combination of auxins and cytokinins are frequently used for *in vitro* production of phenolic compounds, especially flavonoids (Jedinák et al., 2004; Grąbkowska et al., 2016; Fazal et al., 2016; Anjum et al., 2017).

In a previous study, we described the effects of the interaction between auxin-cytokinin and light on calli (Fig. 1C–D) induction and phenolic compounds production in *P. venusta* (Coimbra et al., 2017). In the current study, we evaluated the growth and ultrastructure of the primary callus during culture in order to determine calli morphology and detect cells with embryogenic characteristics. A comparative analysis of bioactive phenolic compounds was performed using an HPLC protocol to identify the production of these compounds throughout the culture.

2. Material and methods

2.1. Chemicals

Agar, chlorogenic, *trans*-cinnamic, ferulic, caffeic and tannic acids, apigenin, rutin, (+)-catechin hydrate, luteolin, chrysin, quercetin, 2,4-dichlorophenoxyacetic acid (2,4-D), 6-benzilaminopurine (BAP), anthrone, 3,5-dinitrosalicylic acid (DNS), glucose, sucrose, Coomassie blue, bovine serum albumin, glycine, ninhydrin, Folin-Ciocalteu reagent, methanol and formic acid were purchased from Sigma-Aldrich Co. (St. Louis, MO, USA).

2.2. Plant material

The explants were obtained from leaves of *Pyrostegia venusta* (Ker Gawl.) Miers (Bignoniaceae) collected in the Brazilian Cerrado region in Divinópolis, Midwest Minas Gerais State, Brazil (20°10′45.9″S and 44°55′07.2″W GRW) (SISBIO no. 24542-6). Fertile samples were collected and the vouchers were identified by Andréia Fonseca Silva of PAMG Herbarium (PAMG 56307) at the Agricultural Research Company of Minas Gerais (EPAMIG). This work was registered in the SisGen Platform (Register A12A940), according to Brazilian Biodiversity Law 13.123/2015. A part of the leaves was used for comparison of the type and amount of the primary and secondary metabolites.

2.3. Callus induction and growth

The explants of *Pyrostegia venusta* were treated with 70% ethanol (1 min), 1% NaClO (5 min) and washed three times in sterilized water. The initial explants (IE) (6 mm) were placed on basal medium MS (Murashige and Skoog, 1962) added of 4.52 μM 2,4-dichlorophenoxiacetic acid (2,4-D) and 8.88 μM 6-benzylaminopurine (BAP), with 30 g L^{-1} sucrose and solidified with 7 g L^{-1} agar (Coimbra et al., 2017). The pH was adjusted to 5.8 ± 0.1 with 0.1 N NaOH, and the medium was sterilized at 120 °C (1.37 × 105 Pa) for 20 min. The explants were transferred to a growth chamber and kept at 27 ± 2 °C in the absence of light. The growth pattern of callus culture was followed using a growth curve with an interval of 10 days, for 120 days, corresponding to the decline phase, according to Smith (2013).

Calli samples were taken to evaluate growth, morphology and primary (soluble proteins, amino acids, soluble and reducing sugars) and secondary metabolite (total phenols and flavonoids) contents. The chromatographic profile of the phenolic compounds also was determined by HPLC for the initial explant and callus with 60 and 120 days. For assessing callus growth, the experimental design was completely randomized consisting of 25 repetitions.

2.4. Ultrastructural analyses

2.4.1. Scanning electron microscopy (SEM)

Fresh callus samples were fixed in Karnovsky's solution (2.5% glutaraldehyde and 2.5% paraformaldehyde) in 0.05 M cacodylate buffer, pH 7.0, for 24 h at 4 °C and prepared according to Pádua et al. (2018). The samples were observed using a LEO EVO-40, PVX scanning electron microscope.

2.4.2. Transmission electron microscopy (TEM)

For analysis in a transmission electron microscope, fresh callus samples were fixed in modified Karnovsky (2.5% glutaraldehyde, 2.0% paraformaldehyde, 0.05 M cacodylate buffer, pH 7.2) for 24 h and prepared according to the protocol described by Bossola and Russell (1999). Semithin (0.85 μm) and ultrathin (< 100 nm) sections were cut using a Reichrt-jung (Ultracut) ultramicrotome and stained with uranyl acetate and lead citrate (Bossola and Russell, 1999). The observations and electrophotographs were performed using a TE microscope Zeiss EM 109 at 80 kV coupled to a Megaview digital camera and captured with iTEM software (Olympus Software Imaging Solutions).

2.5. Primary metabolites profile

2.5.1. Aqueous extracts preparation

Fresh calli (500 mg) were extracted with 4 mL of distilled water at 4 °C using a mortar. The extract was left in a water bath at 40 °C for 30 min and centrifuged at 4800 × *g* for 30 min (Santos et al., 2010). The supernatant was collected and used for analysis of protein, amino acid, reducing and soluble sugar contents. Determinations were performed in triplicate using a Shimadzu UV-1800 spectrophotometer.

2.5.2. Total protein content

The total protein concentration was assessed according to Bradford (1976). The protein content was quantified using a standard curve of bovine serum albumin (BSA, 0–100 μg 100 μL^{-1}), according to Bradford (1976). The result was expressed in milligrams of total protein per gram of fresh matter (mg PT g^{-1} FW).

2.5.3. Amino acid content

The amino acid content was quantified according Stein and Moore (1948). The amino acid concentrations were determined using a glycine standard curve (0–0.10 μmol mL^{-1}). The result was expressed in milligrams of amino acids per gram of fresh matter (mg AA g^{-1} FW).

2.5.4. Total soluble sugar content

The total soluble sugar content was estimated according to Yemm and Willis (1954). The sugar concentration was determined using a standard glucose curve (0–60 μg mL^{-1}). The result was expressed in milligrams of total soluble sugar per gram of fresh matter (mg SS g^{-1} FW).

2.5.5. Reducing sugar content

The reducing sugar content was quantified according to Miller (1959). The sugar concentrations were determined using a standard glucose curve (0–6 μmol mL^{-1}). The result was expressed in milligrams of reducing sugar per gram of fresh matter (mg RS g^{-1} FW).

2.6. Secondary metabolites profiles

2.6.1. Hydromethanolic extract preparation

Dried calli (200 mg) were extracted with 10 mL methanol:water (1:1) with constant stirring for 4 h in ambient temperature using shaker apparatus (Castro et al., 2009). The extract was filtered, and the final volume was made up to 10 mL with methanol:water (1:1).

2.6.2. Total phenols content

Phenols were quantified with 100 μL of hydromethanolic extract, following the AOAC (1995) procedure. The total phenol content was calculated using a calibration curve with 100 μg mL^{-1} tannic acid solution as the standard. Determinations were performed in triplicate, and the result was given in microgram equivalents of tannic acid per milligram of dry matter (μg ATE mg^{-1} DW).

2.6.3. Total flavonoids content

The total flavonoid assay was performed according to Woisky and Salatino (1998), and flavonoid content was calculated using a calibration curve with 100 μg mL^{-1} rutin in a methanol solution of 2% aluminum chloride as standard. Determinations were performed in triplicate, and the result was given in microgram equivalents of rutin per milligram of dry matter (μg RE mg^{-1} DW).

2.6.4. HPLC analysis

Chromatographic profiles were obtained in a modular system liquid chromatography Shimadzu Prominence HPLC (Shimadzu Corp., Kyoto, Japan). The separation of compounds was performed with a reversed-phase column Gemini C18 (4.6 × 250 mm, 5 μm, Phenomenex®, Torrance, CA, USA) conditioned at 35 °C. The best chromatographic conditions were obtained using mobile phases comprising A) water:-formic acid (99.9:0.1) and B) methanol:formic acid (99.9:0.1) at the proportion of 0% B (0–5 min); 0–100% B (5–30 min); 100% B (30–35 min). A 20 μL injection volume and a flow rate of 1.0 mL min^{-1} were employed. Separations were monitored at three wavelengths to detect phenolic compounds; 254 nm and 328 nm for phenolic acids and flavan-3-ols and 350 nm for flavones, flavonols and chalcones (Duarte-Almeida et al., 2006). The determination of phenolic compounds was performed by comparing retention times and UV spectrum of standards previously injected and by data from the literature (Ruiz et al., 2013; Abad-García et al., 2009; Chen et al., 2004; Sakakibara et al., 2003). Three replicates were carried out on the same day.

2.7. Data analysis

The data were subjected to Shapiro-Wilk and Bartlett (χ^2) tests to check the normality and homogeneity of variances, respectively. All variables were normally distributed and the variances were homogeneous. Thus, the data were subjected to F test at $p \leq 0.05$ significance level using the Variance Analysis System of Balanced Data SISVAR 5.1 Software (Ferreira, 2011). Mean rates were further separated by Tukey's Test when differences were significant.

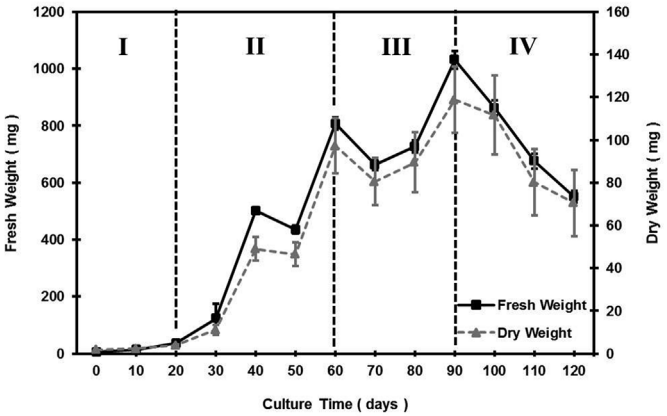

Fig. 2. Callus growth of *Pyrostegia venusta* on MS medium with 4.52 μM 2,4-D and 8.88 μM BAP in absence of light. Data represent the average of 25 replications ± standard deviation (SD). I – *lag* phase (0–20 days), II – exponential phase (21–60 days), III – linear phase (61–90 days), IV – decline phase (91–120 days).

3. Results and discussion

3.1. Calli growth

Callus induction started at seven days after inoculation. Calli grew in a sigmoidal pattern, with four distinct phases: *lag* (0–20th day), exponential (21st to 60th day), linear (61st to 90th day) and decline (91st to 120th day) (Fig. 2), represented by the regression equation $y = 72{,}984x\text{-}15{,}954$ ($R^2 = 0.6632$). There was an accumulation of fresh weight until the 90th day, which progressively increased throughout the culture. The *lag* phase lasted until the 20th day after inoculation, characterized by the accumulation of fresh weight, averaging 0.02 g/callus. In this phase, the calli exhibited a white color. The exponential growth phase extended from the 21st to the 60th day with an intense cell division. In this phase, calli were yellow and friable, with values of fresh weight of 0.47 g/callus on average, and growth of 96% compared to the previous phase. The linear phase was observed between the 61st and 90th days of culture, with fresh weight accumulation of 24% and an average of 0.81 g/callus. At this stage, calli were friable and yellow; however, some samples showed signs of oxidation. There was no stationary phase. From the 91st day, the culture entered the decline phase, characterized by a 16% reduction in the values of fresh weight, relative to the linear phase, averaging at 0.69 g/callus. The calli were friable and predominantly dark yellow, with many oxidized regions. At the end of the experimental period, calli were completely oxidized as a consequence of phenolic oxidation that induces the formation of brown pigments (Sapers et al., 2002).

3.2. Ultrastructural analyses

Analyses carried out using SEM (Fig. 3A–F) showed predominantly small and isodiametric cells with meristematic characteristics, able to multiply. In the first 20 days of culture (*lag* phase), calli presented rounded cells arranged in clusters and some cells in division (Fig. 3A). Some regions with elongated cells also were observed (Fig. 3B). At 20 days of culture, corresponding to the end of the *lag* phase and the beginning of the exponential phase, isodiametric cells with meristematic characteristics predominated, forming clusters of cells (Fig. 3C). During the exponential phase (21–60 days), the calli maintained the previous pattern, with predominance of round cells, but less crowded. Between 61 and 90 days of culture (linear phase), the calli showed numerous compact isodiametric cell masses, similar to pro-embryogenic structures (Fig. 3D). At 90 days, cellular organizations were observed in clusters. The cells presented a membranous layer on the cell surface

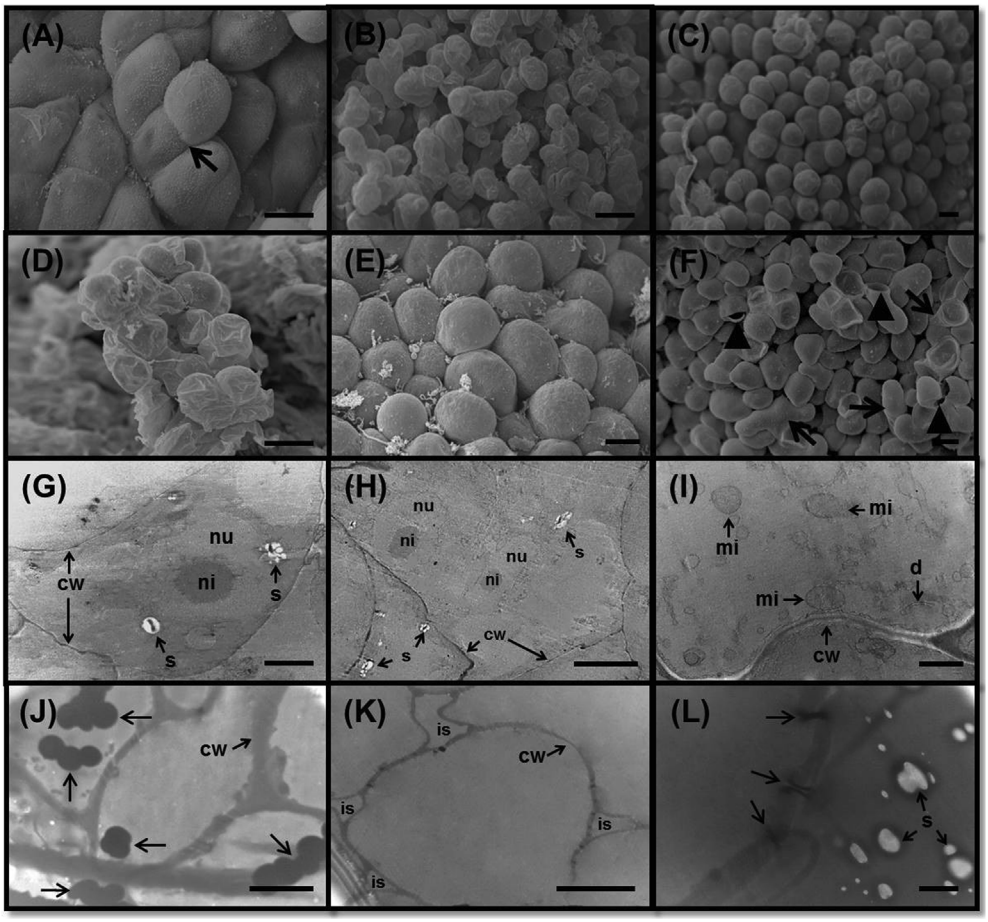

Fig. 3. Scanning (**A-F**) and transmission (**G-L**) electron photomicrographs of *P. venusta* calli. (**A**) *lag* phase – cell in division (arrow); (**B**) *lag* phase – elongated cells; (**C**) exponential phase – isodiametric cells with meristematic characteristics; (**D**) linear phase – cell masse (cluster); (**E**) linear phase – detail of the cluster of cells; (**F**) decline phase – elongated (arrows) and ruptured cells (head arrows); (**G**) *lag* phase cells: see bulky nucleus with prominent nucleolus, starch granules and thin cell wall; (**H**) exponential phase with cells in division; (**I**) linear phase: cells with mitochondria, dictyosome and thick cell wall in detail; (**J**) vacuolated cells at the start of the decline phase with thick cell wall and osmiophilic deposition (arrows); (**K**) vacuolated cells in the decline phase: see the presence of intercellular spaces; (**L**) detail of the cell wall at the end of the decline phase: see the presence of plasmodesmata (arrows) and starch granules. *Abbreviations*: *s* – starch granules; *is* – intercellular spaces; *cw* – cell wall; *mi* – mitochondria; *d* – dictyosome; *nu* – nucleus; *ni* – nucleoli. *Scale bars*: 20 μm (**A-F**); 10 μm (**H,J,K**); 2 μm (**G**); 1 μm (**I,L**).

indicating morphogenic capacity (Fig. 3E). Some ruptured cells were observed, indicating the start of the senescence of culture. In the decline phase, from 91st day of culture, the calli showed mostly elongated and ruptured cells, especially at 120 days of culture (Fig. 3F).

Similar morphology was also found in morphogenic callus of *Actinidia deliciosa* cv. Hayward (Popielarska et al., 2006) and embryogenic callus of *Boesenbergia rotunda* (Ng et al., 2016). In many studies of *in vitro* plant culture, SEM analysis revealed that morphogenesis is linked to the appearance of a fibrillar network, referred to as the extracellular matrix surface network (Šamaj et al., 1995). The chemical composition and structural arrangement of the extracellular matrix surface on the cell surface indicate a fundamental role in cell-to-cell recognition and interaction, cell division and differentiation and also in the generation and maintenance of some traits in plant cell populations (Bobák et al., 2003/4). On the other hand, during preparation of material for SEM observations, critical-point drying may cause shrinkage and hole formation in the extracellular surface layer covering morphogenic cells (Šamaj et al., 1999).

Analysis by TEM (Fig. 3g–l) showed in the *lag* phase, calli cells with dense cytoplasm, large nuclei, small vacuoles, thin cell walls and starch grains (Fig. 3G). These characteristics suggest an intense synthesis of RNA and extensive metabolic activity (Aslam et al., 2011). Starch accumulated in callus cells could provide large amounts of energy required for organ initiation and further development (Forters and Pais, 2000). In the exponential phase, calli cells showed starch grains, large vacuoles, thin cell walls and absence of intercellular spaces (Fig. 3H). In the linear phase, a well-developed nucleus, nucleolus and thin cell walls, apparent dictyosome, vesicles and numerous mitochondria and absence of intercellular spaces were observed (Fig. 3I). The isodiametric shape of the mitochondria is an important characteristic of both high metabolic activity and respiration rate (Kaewubon et al., 2015). From 100 days of culture (decline phase), there were cells in three different stages: 1) cells with a large amount of electron-dense granules (vesicles containing dense pigmentation consisting of a dark osmiophilic material) (Fig. 3J), similar to that observed in the browning callus of *Dendrobium crumenatum* by Kaewubon et al. (2015); 2) fully vacuolated cells without visible organelles (Fig. 3K); and 3) cells with disrupted cell membranes with leakage of cytoplasmic contents, showing the process of cell senescence (Fig. 3L). Thick cell walls, evident intercellular spaces and starch granules were also observed. The presence of large or numerous vacuoles is involved in the cellular degradation process, and the vacuole plays an essential role in the programmed cell death process (Lam et al., 2000; Graner et al., 2015).

Image analysis by SEM and TEM have been used not only to understand embryogenesis and organogenesis *in vitro*, but also for quality control of cell culture (Ibaraki and Kenji, 2001), cytological and cytogenetic events (Fras et al., 2007), cell viability (Herrera et al., 2011; Chiavegatto et al., 2015), programmed cell death (Graner et al., 2015), and browning (Kaewubon et al., 2015). However, the isolated use of SEM and TEM is not enough to clarify these questions.

3.3. Primary metabolites profile

The highest protein and amino acid contents were observed at 10 days of culture corresponding to the *lag* phase and were also higher than those observed in the initial explant (Fig. 4A and B). This result reflects the nutritional status supplied by the mother plant to explant and used to start the callus growth (Santos et al., 2010). After 20 days of culture, in the exponential phase, the total protein content decreased and in general, the total amino acids content remained significantly lower than in the beginning of the culture and in the initial explant ($P < 0.05$). At 70 days of culture, in the linear phase, the calli culture

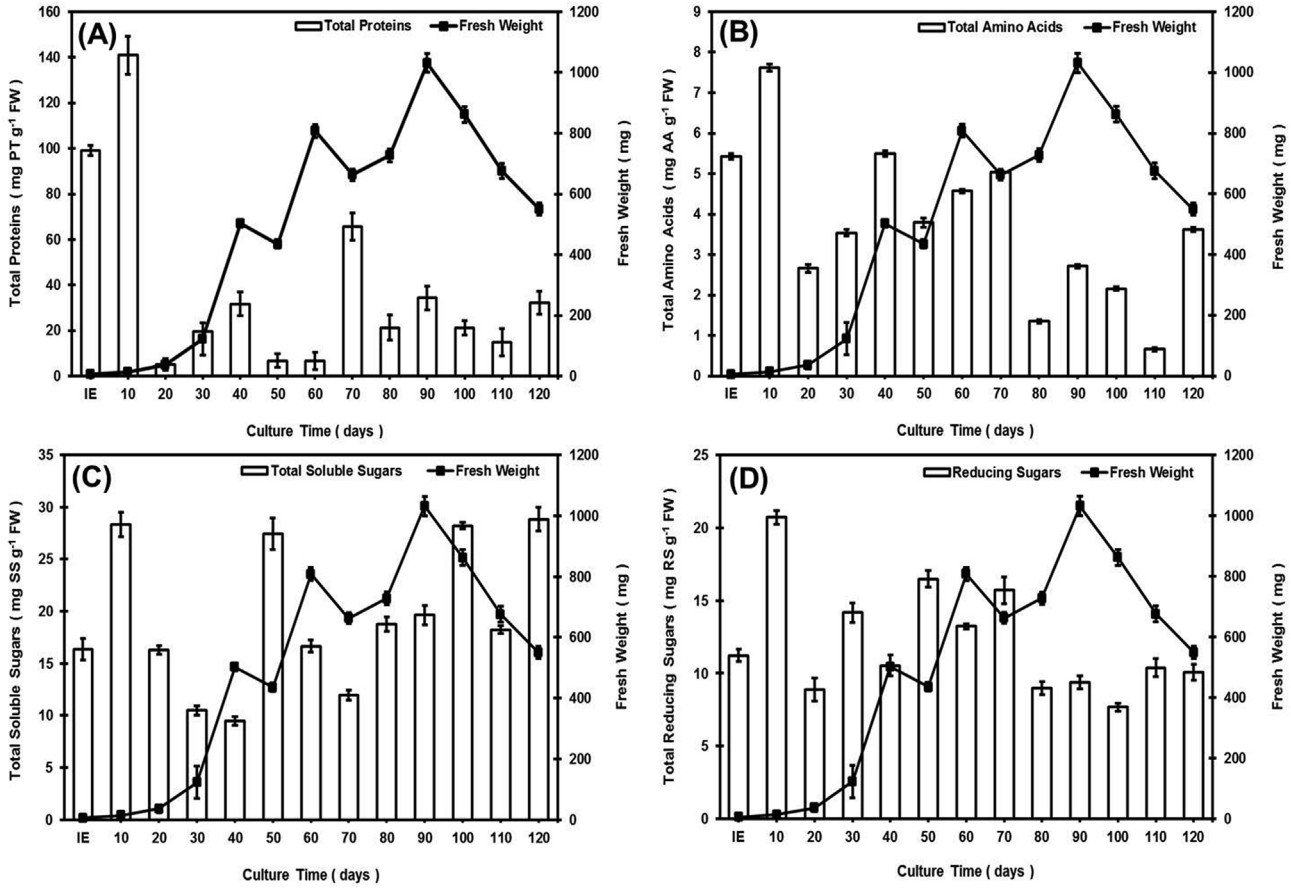

Fig. 4. Primary metabolites contents and fresh weight of the *Pyrostegia venusta* calli. (**A**) Total protein; (**B**) Total amino acids; (**C**) Total soluble sugars; (**D**) Total reducing sugars. Bars show the average of three replicates ± standard deviation. IE – initial explant; PT – proteins; AA – amino acids; SS – soluble sugars; RS – reducing sugars; FW – fresh weight.

exhibited an increase in the total protein content, indicating changes in cell metabolism, which requires specific proteins for the cell expansion and other functions (Costa et al., 2015). From this point, in general, the proteins and total amino acids contents decreased until the decline phase, mainly at 110 days of culture.

Calli showed high soluble and reducing sugar contents at 10 days of culture (*lag* phase) and in general, these contents were higher than in the initial explant during the culture (Fig. 4C and D). The soluble sugar contents oscillated in all the subsequent phases, and high concentrations of these metabolites were observed at 50 days (exponential phase) and 100 and 120 days (decline phase), similar to the 10 days of the *lag* phase ($P < 0.05$) (Fig. 4C). The reducing sugar content remained relatively high throughout the exponential phase and in the beginning of linear phase, at 70 days of culture (Fig. 4D). From this point, the contents decreased until 120 days of culture, corresponding to the decline phase. Increases in sugar content can result in reduced photosynthetic capacity and beginning of the senescence process. The mechanisms involved in the regulation of sugar metabolism and senescence remains unclear. Sugars can trigger a process of autophagy involved in the regression of the cytoplasm, including organelles, and recycling of respiratory substrates (Love et al., 2008).

3.4. Secondary metabolites profile

In general, phenols and flavonoids contents showed an inverse relationship with callus growth, and the highest total phenols and flavonoids contents were observed at 10 days of culture (0.53 and 0.42 $\mu g\, mg^{-1}$ of DW respectively) during the *lag* phase and were also higher than those observed in the initial explant (Fig. 5A and B). Therefore, the contents of these compounds decreased significantly in all subsequent phases (exponential, linear and decline) ($P < 0.05$) and the amounts remained close to the initial explant from 60 to 50 days for the total phenols and flavonoids, respectively. These results indicate that the degree of differentiation of culture affects the biosynthesis of phenolic compounds, as reported in *Schisandra chinensis* by Szopa and Ekiert (2012), where a different accumulation of phenolic acid was found in undifferentiated and organogenic calli. Loredo-Carrillo et al. (2012) suggested that the supplementation of the medium with higher concentrations of sucrose can increase phenolic compounds production in *P. venusta* calli. According to Naik et al. (2010), the decrease in the phenolic compounds contents during callus growth is associated with the consumption of sucrose; so, it is necessary periodic subcultures to renew carbon sources for the construction of new molecules. Phenolic compounds are described as carbon-based secondary compounds, and biochemical and molecular studies strongly support the idea that the levels of carbon-based secondary compounds are positively linked to the contents of available photosynthates (carbon, C) and negatively linked to growth and nutrient status (nitrogen, N) in plants (Nybakken et al., 2011).

Previous studies have also shown the possibility of obtaining high phenolic compounds content *in vitro,* as reported by Diwan et al. (2012) in *Ruta graveolens* (Rutaceae) and Giri et al. (2012) in *Habenaria edgeworthii* (Orchidaceae). The phenolics in the leaves of *P. venusta* have different biological activities and their production is preserved in the callus cultures (Loredo-Carrillo et al., 2012; Braga et al., 2015; Coimbra et al., 2017).

Hydromethanolic extracts from the initial explant and calli at 60 and 120 days of culture were subjected to HPLC for the analysis of

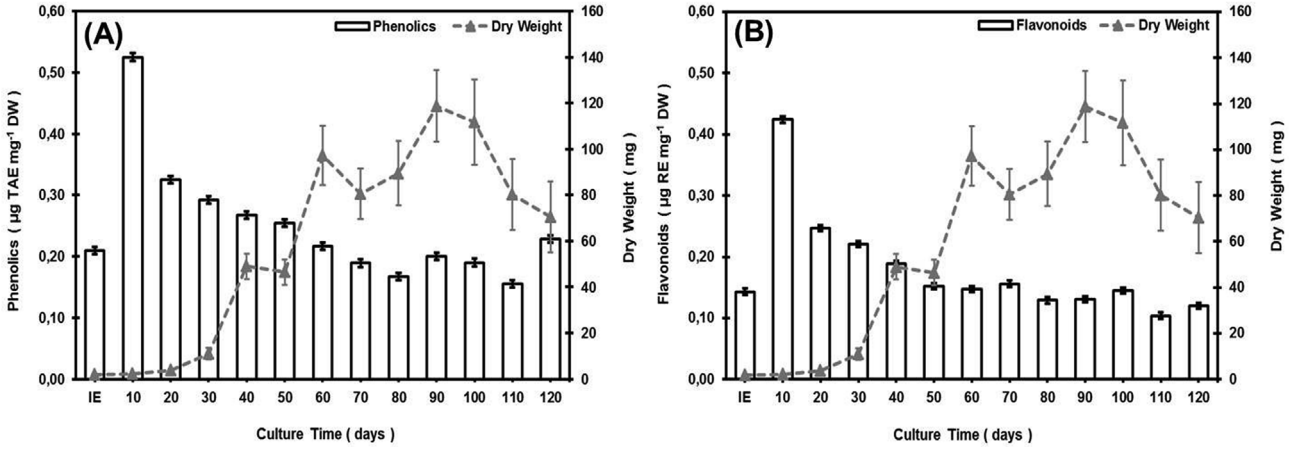

Fig. 5. Secondary metabolites contents and dry weight of the *Pyrostegia venusta* calli. (**A**) Total phenols and (**B**) Total flavonoids. Bars show the average of three replicates ± standard deviation. IE – initial explant; TAE – tannic acid equivalent; RE – rutin equivalent; DW – dry weight.

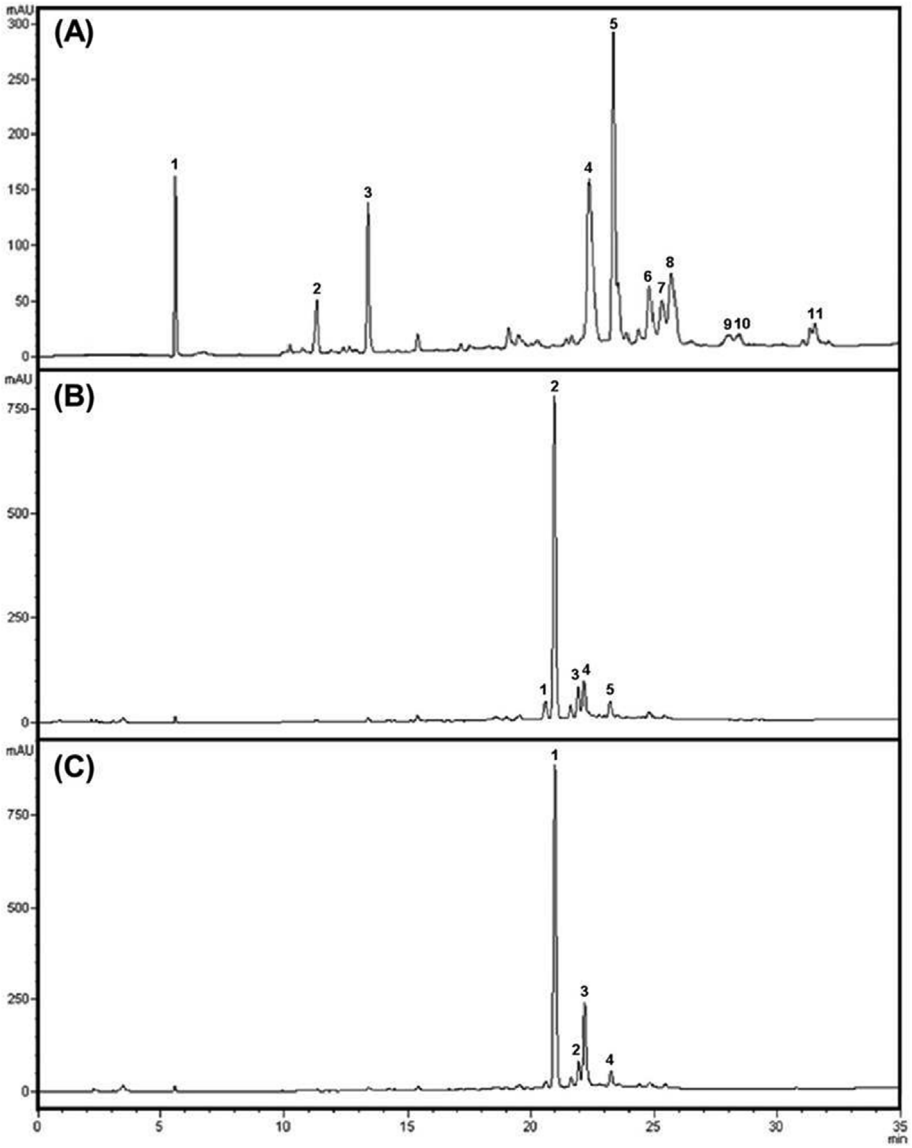

Fig. 6. Profile by high-performance liquid chromatography of the hydromethanolic extracts of *Pyrostegia venusta* calli on MS medium containing 4.52 µM 2,4-D and 8.88 µM BAP. Chromatograms at 254 nm. (**A**) initial explant; (**B**) 60 days of culture; (**C**) 120 days of culture. Peaks 1–3A: benzoic acid derivatives; Peak 4A: *p*-coumaric acid derivative; Peak 5A: rutin; Peaks 6–11A: *p*-coumaric acid derivatives; Peaks 1–5B and 1–4C: caffeic acid derivatives.

phenolic compounds, due to the similarity of the chromatographic profile observed by thin-layer chromatography (data not shown). The analysis of the initial explant and calli indicated the presence of the phenolic acids and flavonoids derivatives (Fig. 6). Results from the initial explant (Fig. 6A) suggested the presence of three benzoic acid derivatives (di- and tri-hydroxylated) (peaks 1–3), seven derivatives from *p*-coumaric acid (peaks 4 and 6–11) and rutin (peak 5). In calli extracts, nine caffeic acid derivatives were detected, with five compounds in calli at 60 days of culture (Fig. 6B) and four compounds in calli at 120 days of culture (Fig. 6C).

A preferential production of caffeic acid derivatives at 60 and 120 days of callus culture were observed. These compounds avoid excessive oxidation and senescence, since caffeic acid and their derivatives are potent scavengers of free radicals and inhibitors of lipidic peroxidation (Olmos et al., 2008). In addition, they have an important role in protecting plants against infections (Leiss et al., 2009). The production of the large variety of phenolic acids in *in vitro* cultures is frequently reported (Szopa et al., 2012, 2013, 2018; Amoo et al., 2017; Szopa and Ekiert, 2012, 2014). Caffeic acid and their derivatives have been widely studied, and there are several studies evidencing their biological activities as anticancer agents (Zeng et al., 2018), and antioxidant (Urbaniak et al., 2017; Marković and Tošović, 2016), cytotoxic, genotoxic and antimicrobial effects (Matejczyk et al., 2018; Shen et al., 2018).

4. Conclusion

The results demonstrate the potential of the *P. venusta* calli as a new source of caffeic acid derivatives. The morphological aspects need to be combined with the phytochemical profile to contribute to the effective characterization of the cultures and aid in the identification of the physiological changes in the callus culture. The *in vitro* production of caffeic acid derivatives encourages further studies to obtain other phenolic compounds of pharmacological and commercial interest.

Acknowledgements

We thank Dr. Andreia Fonseca Silva for the botanical identification of this plant and Dr. Eduardo Alves for providing the Laboratory of Electron Microscopy and Ultra Structural Analysis, Department of Plant Phytopathology/Federal University of Lavras, to perform the analyses under transmission and scanning electron microscopy. The authors also wish to thank to CAPES (Coordination of Improvement of Higher Level Personnel) and FAPEMIG (Foundation for Research Support of Minas Gerais) for financial support.

References

Abad-García, B., Berrueta, L.A., Garmón-Lobato, S., Gallo, B., Vicente, F., 2009. A general analytical strategy for the characterization of phenolic compounds in fruit juices by high-performance liquid chromatography with diode array detection coupled to electrospray ionization and triple quadrupole mass spectrometry. J. Chromatogr. A 1216, 5398–5415.

Amoo, S.O., Moyo, M., Aremu, A.O., Gruz, J., Šubrtová, M., Doležal, K., Van Staden, J., 2017. Cytokinins influence plant regeneration and phenolic acid production in *Hypoxis hemerocallidea* organ and callus cultures. South Afr. J. Bot. 109 325-325.

Anjum, S., Abbasi, B.H., Hano, C., 2017. Trends in accumulation of pharmacologically important antioxidant-secondary metabolites in callus cultures of *Linum usitatissimum* L. Plant Cell Tissue Organ Cult. 129, 73–87.

Aslam, J., Khan, S.A., Cheruth, A.J., Mujib, A., Sharma, M.P., Srivastava, P.S., 2011. Somatic embryogenesis, scanning electron microscopy, histology and biochemical analysis at different developing stages of embryogenesis in six date palm (*Phoenix dactylifera* L.) cultivars. Saudi J. Biol. Sci. 18 (4), 369–380.

Association Official Analytical Chemists, 1995. Official Methods of the Association of Official Analytical Chemists, sixteenth ed. AOAC, Washington.

Bobák, M., Šamaj, J., Hlinková, E., Hlavačka, A., Ovečka, M., 2003/4. Extracellular matrix in early stages of direct somatic embryogenesis in leaves of *Drosera spathulata*. Biol. Plant. 47, 161–166.

Bossola, J.J., Russell, L.D., 1999. Electron Microscopy: Principles and Techniques for Biologists, second ed. Jones and Bartlett Publishers, Boston.

Bradford, M.M., 1976. A rapid and sensitive method for the quantitation of microgram quantities of protein utilizing the principle of protein-dye binding. Anal. Biochem. 72, 248–254.

Braga, K.Q., Coimbra, M.C., Castro, A.H.F., 2015. *In vitro* germination, callus induction and phenolic compounds contents from *Pyrostegia venusta* (Ker Gawl.) Miers. Acta Sci. Biol. Sci. 37, 151–158.

Cardozo, N.P., Parreira, M.C., Alves, P.L., Bianco, S., 2009. Foliar area estimate of two sugarcane-infesting weeds using leaf blade linear dimensions. Planta Daninha 27, 683–687.

Castro, A.H.F., Paiva, R., Alvarenga, A.A., Vítor, S.M.M., 2009. Calogênese e teores de fenóis e taninos totais em barbatimão [*Stryphnodendron adstringens* (Mart.) Coville]. Cienc. E Agrotecnol 33 (2), 385–390.

Chen, X., Kong, L., Su, X., Fu, H., Ni, J., Zhao, R., Zou, H., 2004. Separation and identification of compounds in *Rhizoma chuanxiong* by comprehensive two-dimensional liquid chromatography coupled to mass spectrometry. J. Chromatogr. A 1040, 169–178.

Chiavegatto, R.B., Castro, A.H.F., Marçal, M.G., Pádua, M.S., Alves, E., Techio, V.H., 2015. Cell viability, Mitotic index and callus morphology of *Byrsonima verbascifolia* (Malpighiaceae). Tropical Plant Biol. 8, 87–97.

Coenen, C., Lomax, T.L., 1997. Auxin-cytokinin interactions in higher plants: old problems and new tools. Trends Plant Sci. 2, 351–356.

Coimbra, M.C., Chagas, R.C.R., Duarte-Almeida, J.M., Castro, A.H.F., 2017. Influence of plant growth regulators and light on callus induction and bioactive phenolic compounds production in *Pyrostegia venusta* (Bignoniaceae). Indian J. Exp. Biol. 55 (8), 584–590.

Costa, J.L., Silva, A.L.L., Bier, M.C.J., Brondani, G.E., Gollo, A.L., Letti, L.A.J., Erasmo, E.A.L., Soccol, C.R., 2015. Callus growth kinetics of physic nut (*Jatropha curcas* L.) and content of fatty acids from crude oil obtained *in vitro*. Appl. Biochem. Biotechnol. 176, 892–902.

Diwan, R., Shinde, A., Malpathak, N., 2012. Phytochemical composition and antioxidant potential of *Ruta graveolens* L. *in vitro* culture lines. J. Bot. 2012, 685427 6 pages.

Duarte, M.R., Jurgensen, I., 2007. Morpho-anatomical diagnosis of the leaf and stem of *Pyrostegia venusta* (Ker Gawl.) Miers, bignoniaceae. Lat. Am. J. Pharm. 26 (1), 70–75.

Duarte-Almeida, J.M., Vidal Novoa, A., Lynares, A.F., Lajolo, F.M., Genovese, M.I., 2006. Antioxidant activity of phenolics compounds from sugar cane (*Saccharum officinarum* L.) juice. Plant Foods Hum. Nutr. 61, 187–192.

Fazal, H., Abbasi, B.H., Ahmad, N., Ali, S.S., Akbar, F., Kanwal, F., 2016. Correlation of different spectral lights with biomass accumulation and production of antioxidant secondary metabolites in callus cultures of medicinally important *Prunella vulgaris* L. J. Photochem. Photobiol. B 159, 1–7.

Ferreira, D.F., 2011. SISVAR: a computer statistical analysis system. Ciênc. Agrotec. 35 (6), 1039–1042.

Ferreira, D.T., Alvares, P.S.M., Houghton, P.J., Braz-Flho, R., 2000. Chemical constituents from roots of *Pyrostegia venusta* and considerations about its medicinal importance. Quím. Nova 23, 42–46.

Forters, A.M., Pais, M.S., 2000. Organogenesis from internode-derived nodules of *Humulus lupulus* var. Nugget (Cannabinaceae): histological studies and changes in the starch content. Am. J. Bot. 87 (7), 971–979.

Fras, A., Juchimiuk, J., Siwinska, D., Maluszynska, J., 2007. Cytological events in explants of *Arabidopsis thaliana* during early callogenesis. Plant Cell Rep. 26, 1933–1939.

Giri, L., Dhyani, P., Rawat, S., Bhatt, I.D., Nandi, S.K., Rawal, R.S., Pande, V., 2012. *In vitro* production of phenolic compounds and antioxidant activity in callus suspension cultures of *Habenaria edgeworthii*: a rare Himalayan medicinal orchid. Ind. Crops Prod. 39, 1–6.

Graner, E.M., Brondani, G.E., Almeida, C.V., Batagin-Piotto, K.D., Almeida, M., 2015. Study of senescence in old cultures of the *Bactris gasipaes* Kunth *in vitro*. Plant Cell Tissue Organ Cult. 120, 1169–1189.

Grąbkowska, R., Matkowsk, A., Grzegorczyk-Karolak, I., Wysokińska, H., 2016. Callus cultures of *Harpagophytum procumbens* (Burch.) DC. ex Meisn.; production of secondary metabolites and antioxidant activity. South Afr. J. Bot. 103, 41–48.

Herrera, R.C., Paiva, R., Stein, V.C., Salgado, C.C., Magalhães, M.M., Soares, F.P., 2011. The Mitosis index and cell viability in embryonic calli of murici-pequeno. Rev. Ciencias Agrar. 54, 28–32.

Ibaraki, Y., Kenji, K., 2001. Application of image analysis to plant cell suspension cultures. Comput. Electron. Agric. 30, 193–203.

Isah, T., Umar, S., Mujib, A., Sharma, M.P., Rajasekharan, P.E., Zafar, N., Frukh, A., 2018. Secondary metabolism of pharmaceuticals in the plant *in vitro* cultures: strategies, approaches, and limitations to achieving higher yield. Plant Cell Tissue Organ Cult. 132, 239–265.

Jedinák, A., Faragó, J., Pšenáková, I., Maliar, T., 2004. Approaches to flavonoid production in plant tissue cultures. Biologia 59 (6), 697–710.

Kaewubon, P., Hutadilok-Towatana, N., Silva, J.A.T., Meesawat, U., 2015. Ultrastructural and biochemical alterations during browning of pigeon orchid (*Dendrobium crumenatum* Swartz) callus. Plant Cell Tissue Organ Cult. 121, 53–69.

Lam, E., Fukuda, H., Greenberg, J., 2000. Programmed cell death of tracheary elements as a paradigm in plants. Plant Mol. Biol. 44, 245–253.

Leiss, K.A., Maltese, F., Choi, Y.H., Verpoorte, R., Klinkhamer, P.G.L., 2009. Identification of chlorogenic acid as a resistance factor for thrips in Chrysanthemum. Plant Physiol. 150, 1567–1575.

Loredo-Carrillo, S.E., Santos-Diáz, M.L., Leyva, E., Santos-Diáz, M.S., 2012. Establishment of callus from *Pyrostegia venusta* (Ker Gawl.) Miers and effect of abiotic stress on flavonoids and sterols accumulation. J. Plant Biochem. Biotechnol. 22, 312–318.

Love, A.J., Milner, J.J., Sadanandom, A., 2008. Timing is everything: regulatory overlap in plant cell death. Trends Plant Sci. 13, 589–595.

Marković, S., Tošović, J., 2016. Comparative study of the antioxidative activities of caffeoylquinic and caffeic acids. Food Chem. 210, 585–592.

Matejczyk, M., Świsłocka, R., Golonko, A., Lewandowski, W., Hawrylik, E., 2018. Cytotoxic, genotoxic and antimicrobial activity of caffeic and rosmarinic acids and their lithium, sodium and potassium salts as potential anticancer compounds. Adv. Med. Sci. 63, 14–21.
Miller, G.L., 1959. Use of dinitosalicylic acid reagent for the determination of reducing sugar. Anal. Chem. 31, 426–428.
Moreira, C.G., Horinouchia, C.D.S., Souza-Filho, C.S., Campos, F.R., Barison, A., Cabrini, D.A., Otuki, M.F., 2012. Hyperpigmentant activity of leaves and flowers extracts of *Pyrostegia venusta* on murine B16F10 melanoma. J. Ethnopharmacol. 141, 1005–1011.
Moreira, C.G., Carrenho, L.Z.B., Pawloski, P.L., Soley, B.S., Cabrini, D.A., Otuki, M.F., 2015. Pre-clinical evidences of *Pyrostegia venusta* in the treatment of vitiligo. J. Ethnopharmacol. 168, 315–325.
Murashige, T., Skoog, F., 1962. A revised medium for rapid growth and bio assays with tobacco tissue cultures. Physiol. Plantarum 15, 473–497.
Murthy, H.N., Lee, E.J., Paek, K.Y., 2014. Production of secondary metabolites from cell and organ cultures: strategies and approaches for biomass improvement and metabolite accumulation. Plant Cell Tissue Organ Cult. 118, 1–16.
Naik, P.M., Manohar, S.H., Praveen, N., Murty, H.N., 2010. Effects of sucrose and pH levels on *in vitro* shoot regeneration from leaf explants of *Bacopa monnieri* and accumulation of bacoside A in regenerated shoots. Plant Cell Tissue Organ Cult. 100, 235–239.
Ng, T.L.M., Karim, R., Tan, Y.S., The, H.F., Danial, A.D., Ho, L.S., Khalid, N., Appleton, D.R., Harikrishna, J.A., 2016. Amino acid and secondary metabolite production in embryogenic and non-embryogenic callus of Fingerroot Ginger (*Boesenbergia rotunda*). PLoS One 11 (6) e0156714.
Nybakken, L., Sandvik, S.M., Klanderud, K., 2011. Experimental warming had little effect on carbon based secondary compounds, carbon and nitrogen in selected alpine plants and lichens. Environ. Exp. Bot. 72 (3), 368–376.
Olmos, A., Giner, R.M., Recio, M.C., Rios, J.L., Gil-Benso, R., Máñez, S., 2008. Interaction of dicaffeoylquinic derivatives with peroxynitrite and other reactive nitrogen species. Arch. Biochem. Biophys. 475, 66–71.
Pádua, M.S., Paiva, L.V., Labory, C.R.G., Alves, E., Stein, V.C., 2013. Induction and characterization of oil palm (*Elaeis guineensis* Jacq.) pro-embryogenic masses. An. Acad. Bras. Ciênc. 85, 1545–1556.
Pádua, M.S., Santos, R.S., Labory, C.R.G., Stein, V.C., Mendonça, E.G., Alves, E., Paiva, L.V., 2018. Histodifferentiation of oil palm somatic embryo development at low auxin concentration. Protoplasma 255, 285–295.
Piza, I.M.T., Lima, G.P.P., Brasil, O.G., 2003. Peroxidase activity and protein levels in micropropagated pineapple plants in saline. Rev. Bras. Agrociênc. 9 (4), 361–366.
Popielarska, M., Ślesak, H., Goralski, G., 2006. Histological and SEM studies on organogenesis in endosperm-derived callus of kiwifruit (*Actinidia deliciosa* cv. Hayward). Acta Biol. Cracov. Ser. Bot. 48 (2), 97–104.
Ribeiro, L.O., Paiva, L., Pádua, M.S., Santos, B.R., Alves, E., Stein, V.C., 2012. Morphological and ultrastructural analysis of various types of banana callus, cv. Prata anã. Acta Sci., Agron. 34 (4), 423–429.
Rossatto, D.R., Kolb, R.M., 2010. Germination of *Pyrostegia venusta* (Bignoniaceae), seed viability and post-seminal development. Braz. J. Bot. 33 (1), 51–60.
Roy, P., Amdekar, S., Kumar, A., Singh, V., 2011. Preliminary study of the antioxidant properties of flowers and roots of *Pyrostegia venusta* (Ker Gawl.) *Miers*. BMC Complement Altern. Med. 11, 69–77.
Roy, P., Amdekar, S., Kumar, A., Singh, R., Sharma, P., Singh, V., 2012. *In vivo* antioxidative property, antimicrobial and wound healing activity of flower extracts of *Pyrostegia venusta* (Ker Gawl.) *Miers*. J. Ethnopharmacol. 140, 186–192.
Ruiz, A., Mardones, C., Vergara, C., Hermosín-Gutiérrez, I., Von Baer, D., Hinrichsen, P., Rodriguez, R., Arribillaga, D., Dominguez, E., 2013. Analysis of hydroxycinnamic acids derivatives in calafate (*Berberis microphylla* G. Forst) berries by liquid chromatography with photodiode array and mass spectrometry detection. J. Chromatogr. A 1281, 38–45.
Sakakibara, H., Honda, Y., Nakagawa, S., Ashida, H., Kanazawa, K., 2003. Simultaneous determination of all polyphenols in vegetables, fruits, and teas. J. Agric. Food Chem. 51, 571–581.
Šamaj, J., Bobák, M., Blehová, A., Krištin, J., Auxtová-Šamajová, O., 1995. Developmental SEM observations on an extracellular matrix in embryogenic calli of *Drosera rotundifolia* and *Zea mays*. Protoplasma 186, 45–49.
Šamaj, J., Baluška, F., Bobák, M., Volkmann, D., 1999. Extracellular matrix surface network of embryogenic units of friable maize callus contains arabinogalactanproteins recognized by monoclonal antibody JIM4. Plant Cell Rep. 18, 369–374.
Santos, D.N., Nunes, C.F., Pasqual, M., Valente, T.C.T., Oliveira, A.C.L., Silveira, N.M., 2010. Biochemical analysis of callus from physic nut. Ciência Rural. 40, 2268–2273.
Santos, A.V., Arrigoni-Blank, M.F., Blank, A.F., Diniz, L.E.C., Fernandes, R.M.P., 2011. Biochemical profile of callus cultures of *Pogostemon cablin* (Blanco) Benth. Plant Cell Tissue Organ Cult. 107, 35–43.
Sapers, G.M., Hicks, K.B., Miller, R.L., 2002. Antibrowning agents. In: Brane, A.L., Davidson, P.M., Salminen, S., Thorngate IIIJ.H. (Eds.), Food Additives, second ed. Marcel Dekker, New York, pp. 543–561.
Scalon, S.P., Vieira, M.C., Lima, A.A., Souza, C.M., Mussury, R.M., 2008. Pregerminative treatments and incubation temperatures on the germination of “cipó-de-São-João” [*Pyrostegia venusta* (Ker Gawl.) Miers] - Bignoniaceae. Rev. Bras. Plantas Med. 10, 37–42.
Shen, J., Wang, G., Zuo, J., 2018. Caffeic acid inhibits HCV replication via induction of IFNα antiviral response through p62-mediated Keap1/Nrf2 signaling pathway. Antivir. Res. 154, 166–173.
Silva, P.B., Medeiros, A.C.M., Duarte, M.C.T., Ruiz, A.L.T.G., Kolb, R.M., Frei, F., Santos, C., 2011. Evaluation of allelopathic potential, antimicrobial and antioxidant activities of *Pyrostegia venusta* (Ker Gawl.) *Miers* (Bignoniaceae) leaf organic extracts. Rev. Bras. Plantas Med. 13, 447–455.
Smith, R.H., 2013. Plant Tissue Culture: Techniques and Experiments, third edn. Academic Press Elsevier, New York.
Stein, W., Moore, S., 1948. A modified ninhydrin reagent for photometric determination of amino acids and related compounds. J. Biol. Chem. 176, 367–372.
Szopa, A., Ekiert, H., 2012. *In vitro* cultures of *Schisandra chinensis* (Turcz.) Baill. (Chinese magnolia vine) - a potential biotechnological rich source of therapeutically important phenolic acids. Appl. Biochem. Biotechnol. 166, 1941–1948.
Szopa, A., Ekiert, H., 2014. Production of biologically active phenolic acids in *Aronia melanocarpa* (Michx.) Elliott *in vitro* cultures cultivated on different variants of the Murashige and Skoog medium. Plant Growth Regul. 72, 51–58.
Szopa, A., Ekiert, H., Szewczyk, A., Fugas, E., 2012. Production of bioactive phenolic acids and furanocoumarins in *in vitro* cultures of *Ruta graveolens* L. and *Ruta graveolens* ssp. *Divaricate* (Tenore) Gams. under different light conditions. Plant Cell Tissue Organ Cult. 110, 329–336.
Szopa, A., Ekiert, H., Muszynska, B., 2013. Accumulation of hydroxybenzoic acids and other biologically active phenolic acids in shoot and callus cultures of *Aronia melanocarpa* (Michx.) Elliott (black chokeberry). Plant Cell Tissue Organ Cult. 113, 323–329.
Szopa, A., Kubica, P., Snoch, A., Ekiert, H., 2018. High production of bioactive depsides in shoot and callus cultures of *Aronia arbutifolia* and *Aronia* × *prunifolia*. Acta Physiol. Plant. 40 (3), 1–11.
Urbaniak, A., Kujawski, J., Czaja, K., Szelag, M., 2017. Antioxidant properties of several caffeic acid derivatives: a theoretical study. C. R. Chim. 20, 1072–1082.
Veloso, C.C., Bitencourt, A.D., Cabral, L.D.M., Franqui, L.S., Dias, D.F., Santos, M.H., Soncini, R., Giusti-Paiva, A., 2010. *Pyrostegia venusta* attenuate the sickness behavior induced by lipopolysaccharide in mice. J. Ethnopharmacol. 132, 355–358.
Veloso, C.C., Cabral, L.D.M., Bitencourt, A.D., Franqui, L.S., Santa-Cecília, F.V., Dias, D.F., Soncini, R., Vilela, F.C., Giusti-Paiva, A., 2012. Anti-inflammatory and anti-nociceptive effects of the hydroethanolic extract of the flowers of *Pyrostegia venusta* in mice. Braz. J. Pharmacogn. 22, 162–168.
Veloso, C.C., Oliveira, M.C., Oliveira, C.C., Rodrigues, V.G., Giusti-Paiva, A., Teixeira, M.M., Duarte, I.D., Ferreira, A.V.M., Perez, A.C., 2014. Hydroethanolic extract of *Pyrostegia venusta* (Ker Gawl.) Miers flowers improves inflammatory and metabolic dysfunction induced by high-refined carbohydrate diet. J. Ethnopharmacol. 151, 722–728.
Woisky, R.G., Salatino, A., 1998. Analysis of propolis: some parameters and procedures for chemical quality control. J. Apicult. Res. 37, 99–105.
Yemm, E.W., Willis, A.J., 1954. The estimation of carbohydrates in plant extracts by anthrone. Biochem. J. 57, 508–514.
Zeng, N., Hongbo, T., Xu, Y., Wu, M., Wu, Y., 2018. Anticancer activity of caffeic acid n-butyl ester against A431 skin carcinoma cell line occurs via induction of apoptosis and inhibition of the mTOR/PI3K/AKT signaling pathway. Mol. Med. Rep. 17 (4), 5652–5657.